Synthesis, Spectroscopic Characterization and Antibacterial Assessment of Zirconium(II) and Palladium(II) Complexes of Tetracycline-Salicylaldehyde Mixed Ligand

R.K. Dev[ID], A. Bhattarai[*,ID], N.K. Chaudhary[ID] and P. Mishra[ID]

Bio-inorganic and Materials Chemistry Research Laboratory, Department of Chemistry, Tribhuvan University, M.M.A.M. Campus, Biratnagar, Nepal

*Corresponding author: E-mail: bkajaya@yahoo.com

Zirconium(II) and palladium(II) mixed ligand metal complexes were synthesized by using an equimolar mixture of tetracycline (Tc) as primary ligand and salicylaldehyde as secondary ligand. The metal complexes were characterized by physico-chemical and spectroscopic techniques like CHN analysis, surface tension, pH, conductivity and melting point measurements. The spectroscopic characterization technique includes IR, (^{1}H & ^{13}C) NMR, UV/visible and Mass spectrometry methods. The SEM technique determines the surface morphology of the complexes. The thermal and kinetic stability of the complexes was obtained from TGA/DTA curves from which the parameters like E^*, ΔH^*, ΔS^* and ΔG^* have been calculated by using the Coats-Redfern equation. Molecular modeling gives a geometry of the complex which was obtained from Chem 3D Pro. 12.0 software program. The metal complexes of Zr-TcSal and Pd-TcSal have coordinated with tetrahedral and square planar geometry, respectively. The antibacterial susceptibility study of the synthesized metal complexes was done by Kirby-Bauer paper disc diffusion techniques on *S. aureus*, *E. coli* and *P. aeruginosa* clinical pathogens.

Keywords: Tetracycline, Metal complexes, Thermal analysis, Antibacterial activity.

INTRODUCTION

Since immemorial times, antibiotics have been used to cure the diseases of animals and human beings. Most of the antibiotics cannot be completely absorbed by the animals and humans due to their soluble nature. Nearly 90% prototype or metabolites of antibiotics are released out to the soil and water through manures or urine of patients, resulting in some degradation to the environment. Human utilization of animals' food and food products which have antibiotic residues causes chronic poisoning which results in mutation, cancer and embryotoxicity [1]. Metal compelxes of mixed ligands have wide applications in the field of engineering, science and technology, hydrometallurgy, dyeing, analytical chemistry, textiles as well as in chemotherapy [2]. They are also used as antibacterial, antifungal, antitumor, antipyretic, antimitotic, antimetabolites, antithyroid, antiviral, anti-inflammatory and surface anesthesia activity [3]. The organometallic complexes of mixed ligand formed by the refluxation of the equimolar ratio of primary and secondary ligand along with their metal salts have been a

global interest for the researchers in the field of complexation. Transition metals of carbonyl derivatives are also used as intermediates in the synthesis of very useful organometallic complexes which has huge application in catalysis of reactions such as hydrogenation, epoxidation, carbonylation and hydro-formylation [4]. In metal complexes, the ligand containing the O & N donor atom possesses great importance due to their binding nature with metal atoms. The existence of amine (-NH$_2$) and carboxyl (COO$^-$) group in ligand also serves as a source of N/O donating groups which results in the formation of metal complexes of mixed ligands [5]. Biologically active compounds with metal interaction can be used as a specific goal to improve their activity and overcome their resistance [6]. Tetracyclines (TCs) are one of the most widely applied antibiotics in the field of coordination and medicinal chemistry. Today the cause of increasing antibiotic resistance of microorganisms and on plant development is due to misuse and overdose of antibiotics used by the human being [7]. Tetracycline contains the number of substitution patterns and significant structure deviation can change the antibacterial potency [8]. In this work,

we focused on the preparation of metal complexes of zirconium(II) and palladium(II) by using tetracycline as primary ligand and salicylaldehyde as the secondary ligand. Besides their physico-chemical microanalysis and spectroscopic characterizations, antimicrobial susceptibility test was done by Kirby-Bauer paper disc diffusion techniques using clinical pathogenic bacteria like *S. aureus*, *E. coli* and *P. aeruginosa*.

EXPERIMENTAL

The analytical research-grade (AR) chemicals and solvents were used for the experimental work and purified according to the standard process. Drugs such as tetracycline (Sigma-Aldrich), salicylaldehye, $ZrOCl_2 \cdot 8H_2O$ (Loba Chemie Pvt. Ltd.), MHA and $PdCl_2$ (Himedia) were used during the research and triple distilled water and double-distilled ethanol were used for the experiment.

Elemental microanalysis (C, H, N) of the metal complexes was carried out in Euro-EA 3000 microanalyzer. The UV/visible spectra of the complexes in the DMSO solvent were recorded on Varian, Cary 5000 in the range of 800-260 nm. FT-IR spectral analysis was carried on Perkin Elmer Spectrum II as KBr pellets technique in the range of 4000-400 cm^{-1}. The ^1H NMR was carried out in the presence of DMSO-d_6 solvents on Bruker AvII- 400 MHz Spectrometer and Me_4Si which acts as the internal reference. The kinetic and thermal analysis (TGA/DTA) was carried out under the nitrogen atmosphere at room temperature in the range of 40-750 °C at the linear heating rate of 10 °C min^{-1}. ESI-MS evaluation has been determined through a water UPLC-TQD mass spectrometer in the mass range of 0-1000 *m/z*. The melting point was recorded in VEEGO ASD-10013 programmable melting point apparatus. The surface morphology was done on the JEOL model JSM-6390 LV SEM technique. Molecular modeling of metal complexes was optimized through Chem 3D Pro 12.0 program. Conductance measurement was done in autoranging conductivity/TDS meter TCM 15 +. The pH was recorded from Elico LI 613 pH meter. The antibacterial susceptibility test was carried out by Kirby Bauer's paper disc diffusion technique against clinical pathogens, which was done at the Microbiological Laboratory, Mahendra Morang Adarsh Multiple Campus, Biratnagar, Morang, Nepal.

Antibacterial sensitivity assay: Synthesized metal complexes of mixed ligand have been screened for their antibacterial susceptibility test by Kirby-Bauer paper disc diffusion method on two bacterial strains *i.e.* Gram-negative (*Escherichia coli* and *Pseudomonas aeruginosa)* and Gram-positive *(Staphylococcus aureus)*. Test solutions of the metal complexes were prepared in 30% DMSO at four different concentrations (25, 12.5, 6.25 and 3.125 µg/µL) to measure their actual effectiveness. Firstly, the fresh culture of organisms was prepared in nutrient broth and incubating them for 2 h at 37 °C for their complete and total growth. Blank paper discs were prepared from filter paper (Whatman number1) of 5 mm diameter in size and were sterilized and loaded with test solutions. The sterile MHA (Muller Hinton Agar) media was prepared for antibacterial sensitivity according to their reported literature. The revived and fresh pathogens were slowly swabbed into the sterile media and complexes of different concentrations

were added into the paper disc. The positive control standard antibiotic discs (Amikacin) of 30 mcg/disc were also applied during the tests. After completing all these activities, the loaded Petri plates were kept in an incubator for about 37 °C up to 36 h to observe the zone of inhibition for the bacterial growth [9]. The diameter of zone of inhibition (mm) was visualized through Hi Antibiotic Zone Scale-C.

Synthesis of zirconium complex (Zr-TC/Sal): A solution of primary ligand tetracycline (0.8892 g, 2 mmol) in 70% double distilled ethanol and a solution of $ZrOCl_2 \cdot 8H_2O$ (0.6446 g, 2 mmol) in water was stirred in a magnetic stirrer separately in 50 mL round bottom flask for 4 h and added to the tetracycline solution in dropwise condition. The reaction mixture was further stirred for a few hours more and further added with well-stirred secondary ligand salicylaldehyde (0.2 mL, 2 mmol) dissolved in ethanol. The reaction mixture was further stirred for a few hours and filtered. The filtered reaction mixture was refluxed for 8 h and pH was maintained at 7 by adding 2 N NH_4OH solution and left the beaker for 2 days without any disturbance. As a result, the precipitate was obtained and then filtered, washed with ethanol and water several times and dried. The dried precipitate was recrystallized from ethanol to obtain the black crystals of the zirconium complex (**Scheme-I**).

Synthesis of palladium complex (Pd-TC/Sal): A solution of primary ligand tetracycline (0.8897 g, 2 mmol) in 70% double distilled ethanol and a solution of $PdCl_2$ (0.0893 g, 0.5 mol) in aqueous ethanolic solution was stirred in a magnetic stirrer separately in 50 mL round bottom flask for 4 h. The reaction mixture was further stirred for a few hours more and further added with well-stirred secondary ligand salicylaldehyde (0.2 mL, 2 mmol) dissolved in ethanol. The reaction mixture was further stirred for a few hours and filtered. The filtered reaction mixture was refluxed for 8 h and pH was maintained at 6.7 by adding 2 N NH_4OH solution and left in the beaker for 2 days without any disturbance. As a result, the precipitate was obtained and then filtered, washed with ethanol and water several times and dried. The dried precipitate was recrystallized from ethanol to obtain the black crystals of palladium complex (**Scheme-I**).

RESULTS AND DISCUSSION

Physical characterization: Both metal complexes of zirconium(II) and palladium(II) were obtained as coloured solid by the reaction of primary ligand tetracycline (Tc) and secondary ligand (salicylaldehyde). The experimental data of elemental microanalysis and physico-chemical parameters such as melting point, colour change, electronic absorption of the metal complexes show good agreement with the calculated data and denotes the precise relationship to a molecular formula of the proposed complex (Table-1). The synthesized complexes are solid, higher melting points, generally stable around at room temperature and insoluble in water but soluble in common organic solvents like DMSO. The pH, density, viscosity, surface tension, conductivity of complexes obtained was 6.43 & 5.78, 1.048 & 1.076 (g/mL), 16.99 & 22.50 (cp), 56.30 & 57.50 (mN/m) and 14.70 & 17.80 (µS/cm) respectively for Zr-complex and Pd-complex and determines their non-electrolytic nature.
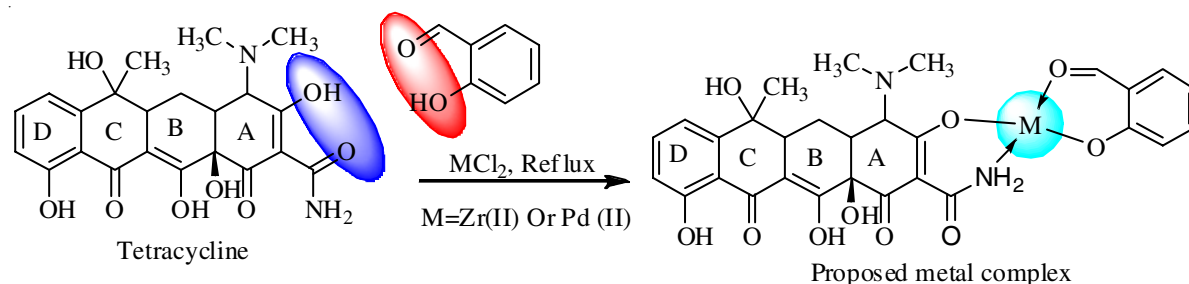
Scheme-I: Synthesis of zirconium(II) and palladium(II) metal complexes of TcSal mixed ligand [tetracycline (Tc) as primary ligand and salicylaldehyde (Sal) as secondary ligand]

TABLE-1
ELEMENTAL MICROANALYSIS, ELECTRONIC ABSORPTION AND PHYSICAL CALCULATION DATA

Complex	m.f.	m.w.	Colour	m.p. (°C)	Elemental analysis (%): Calcd. (found)				UV/vis peak (nm)	Assignment
					C	H	N	O		
Zr-TcSal	$C_{29}H_{28}N_2O_{10}Zr$	655.76	Black	175.9	53.12 (53.06)	4.30 (4.26)	4.27 (4.26)	24.40 (24.39)	268 342 446	$\pi \to \pi^*$ $n \to \pi^*$
Pd-TcSal	$C_{29}H_{28}N_2O_{10}Pd$	670.96	Black	265.5	51.91 (51.87)	4.21 (4.17)	4.18 (4.17)	23.85 (23.84)	263 307 343	$\pi \to \pi^*$ $n \to \pi^*$

FT-IR spectroscopy: The frequencies of FT-IR absorption spectra for zirconium and palladium complexes of mixed ligand was done from the range between 4000-400 cm^{-1}. The bands in the infrared spectrum signify the functional groups attached with the metal ions and also gives important information regarding the coordination sites which are involved during chelation. Broadbands within range of 3407-3183 cm^{-1} were attributed to coalesce of ν(OH/N-H) [10,11]. The bands between 1773-1653 cm^{-1} indicate ν(C=O). Similarly, the sharp IR bands in between 1635-1619 cm^{-1} signify the ν(C=N) which supports that the above complexes are azomethine derivatives [12]. The absorption peaks at 1580-1528 cm^{-1} and 1404-1399 cm^{-1} are due to ν_{asym}(COO$^-$) and ν_{sym}(COO$^-$). Similarly, the appearance of absorptions in the regions 1177-1126 cm^{-1} denotes ν(C-O). Here the coordination of azomethine nitrogen on a metal atom is confirmed by the presence of a new band at 604-602 cm^{-1} and 476-470 cm^{-1} are due to ν(M–O) and ν(M–N), respectively [13,14]. The FT-IR spectrum in combination with other spectral studies signifies the coordination of metal ions to the nitrogen atom of amide group (Table-2).

^{1}H & ^{13}C NMR analysis: The ^{1}H NMR spectra of metal complexes was done in DMSO-d_6 solvent and gives the fruitful information of different proton environments as well as possible coordination sites to metal complexes. Their integral intensity of each signal was found to agree with the number of different types of protons present. The ^{1}H NMR spectrum of the Zr(II) complex, the peak signals at (δ = 2.478-2.495 ppm) revealing to (CH$_3$) and singlet peak appeared at (δ = 2.491-2.523 ppm) is assigned to DMSO-d_6. Similarly, the peaks in the region

of (δ = 2.5-3.5 ppm) represent [N-(CH$_3$)$_2$]. The aromatic proton lies in the location of (δ = 6.950-6.991 ppm) and primary amide proton lies in the vicinity between (δ = 10.214 ppm). Similarly in the palladium(II) complex, the peak signals at (δ = 1.059-1.226 ppm) signify (CH$_3$), (δ = 1.527-1.544 ppm) as (CH$_2$NH) group and (δ = 3.51 ppm) as -OH respectively [15,16].

In the ^{13}C NMR spectra of zirconium metal complexes, the DMSO-d_6 solvent displays chemical shifts at 39.166-40.832 ppm and N(CH$_3$)$_2$ at 45.5 ppm. The aromatic ring carbon confirmed a signal in the range between 113.635-126.652 ppm while the carbonyl group (-CO-) appears in the region of 182.917 ppm. Similarly, palladium complex contains the chemical shift at the region of 40 ppm is due to DMSO-d_6 solvent and the aromatic carbon ring lies at 134.539-137.972 ppm [17].

ESI-Mass analysis: The metal complex of Zr(II) and Pd(II) displays the prominent peak of molecular ion (M$^+$) at (m/z = 656) and (m/z = 671) amu of the parent ion and the base peak appears in m/z = 445 & m/z = 171 region indicates the proposed formula for the complexes. The molecular mass and other spectral data are essential for the generation of the structure of organic compounds. The rest peak in the mass spectrum is the fragment ion peaks. The successive decrease in the peak of the target compounds gives the peak of various fragments and intensities provide stability of fragments ions. The mass spectrum of metal complexes is shown in Fig. 1.

Electronic absorption: The electronic absorption spectroscopy tool is used for distinguishing the characterization for identifying the binding mode of complexes [18]. The spectra

TABLE-2
FT-IR SPECTRAL DATA OF Cd AND Mo-TcSal METAL COMPLEXES

Complex	ν(O-H) or ν(N-H)	ν(C=O)	ν(C=N)	ν_{asym}(COO$^-$)	ν_{sym}(COO$^-$)	ν(C–O)	ν(M–O)	ν(M–N)
Tc Ligand	3384	1653	1615	1580	1399	1126	–	–
Zr-TcSal	3183	1770	1619	1570	1399	1152	604	476
Pd-TcSal	3407	1773	1635	1528	1402	1177	602	470
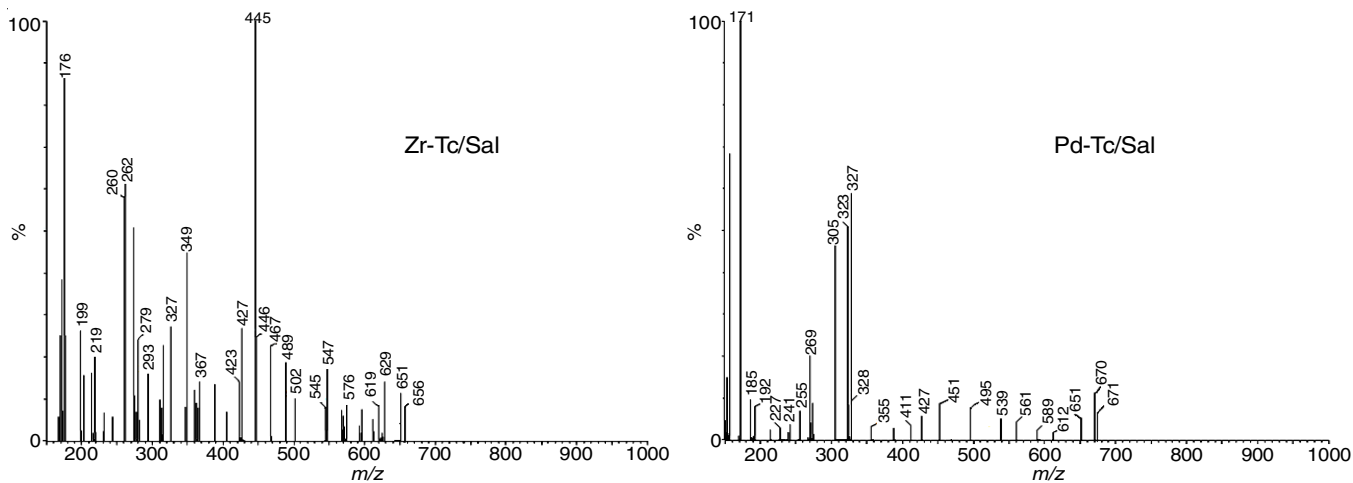
Fig. 1. Mass spectra of zirconium(II) and palladium(II) complexes of TcSal mixed ligand

were taken in a DMSO solvent within a range between 250-800 nm wavelength and are shown in Fig. 2. The electronic spectrum of Zr complex shows excessive-high intense absorption band at 268 and 342 nm, which signify ($\pi \rightarrow \pi^*$) transitions
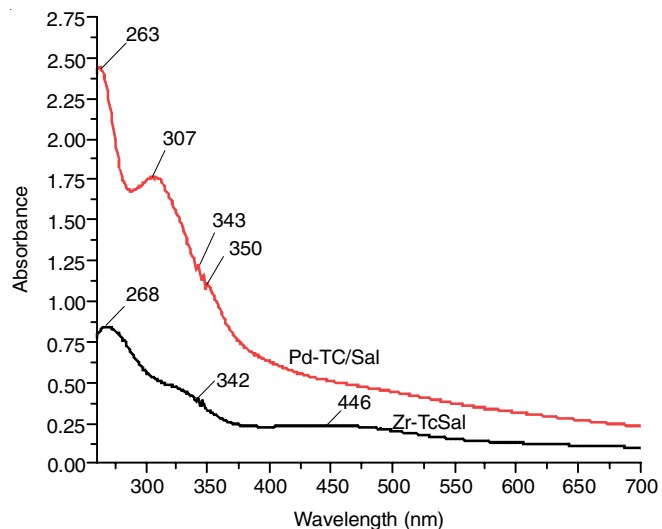
Fig. 2. Electronic absorption spectra of Zr and Pd-TC/Sal metal complex of mixed ligand

of aromatic ring and remains unchanged in zirconium complex and next band at 446 nm signify (n$\rightarrow\pi^*$) transition of >C=N– chromophore and denotes bathochromic shift in zirconium complex arise because of coordination of zirconium metal ion with azomethine nitrogen. The following band moves slightly higher-energy due to polarization of electron interaction of zirconium with >C=N chromophore. Hence due to their d° electronic configuration, there are no *d-d* transitions in Zr(IV) complexes [13,14]. Zirconium complex has been assigned for tetrahedral geometry. Similarly, the electronic spectrum of the Pd-Tc/Sal complex possesses three absorption bands near 263, 307, 343 nm in the visible region. All bands of these types are assigned to have ($\pi\rightarrow\pi^*$) and (n$\rightarrow\pi^*$) transition which specifies the square planar geometry [19].

Thermal analysis: Thermogram of zirconium complex (Fig. 3) has been shown that decomposition takes place in three steps at the temperature between 50.7-755.48 °C. In the first decomposition stage, weight loss of 27.93% (-5.9503 mg) in the temperature range 50.7-108.05 °C. The second and third decomposition steps occurred with % weight loss of 40.60% (1.197 mg) and 83.89% (2.3386 mg) within the temperature range of 249.28-302.03 °C and 633.79-755.48 °C. In each case, decomposition starts with the loss of coordinated or crystallized
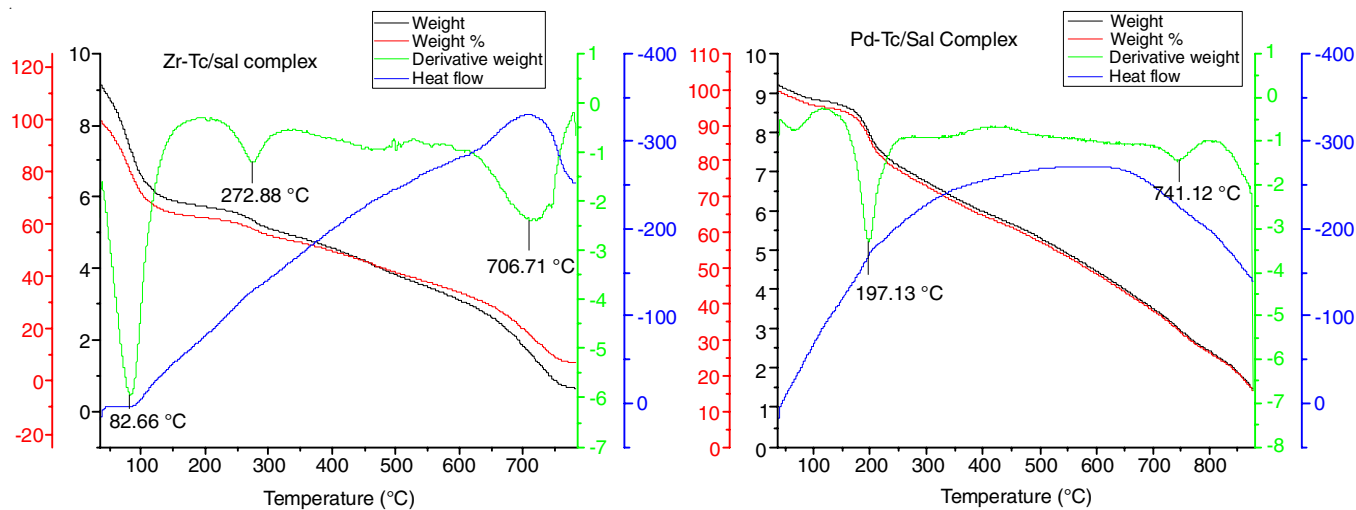
Fig. 3. Thermogram of zirconium and palladium complex

water molecules of the metal complexes only or other components of ligand moiety which confirms the composition of metal complexes. This suggests that zirconium complex is thermally stable. Similarly, thermogram of palladium complex (Fig. 3) was decomposed at two ranges in the temperature range of 164.01-769.19 °C. In the first decomposition stage, weight loss of 20.60% (-3.3048 mg) takes place within the temperature range of 164.01-247.37 °C. The second decomposition stages occur with a mass loss of 65.59% (-1.4339 mg) in the temperature range of 709.75-769.19 °C. The residue formed was metal oxide such as ZrO and PdO.

Kinetic parameters: The kinetic and thermodynamic parameters of the complexes were extracted by making calculation through Coats-Redfern equation. The thermal stability and kinetic parameters of different decomposition steps were calculated and plotted graphically by using the Coats-Redfern relation:

$$\ln\left(-\frac{\ln(1-\alpha)}{T^2}\right) = \ln\left(\frac{AR}{\beta E^*}\right) - \frac{E^*}{RT}$$

here α denotes decomposition fraction at temperature (K) and β signify linear heating rate (dT/dt). A and E^* represent the Arrhenius pre-exponential factor and activation energy. R denotes universal gas constant. Using the equation: y = mx + c, a linear plot of left-hand side *versus* 1/T, whose slope E^*/R gives the activation energy. The other kinetic parameters such as entropy of activation (ΔS^*), enthalpy of activation (ΔH^*) and free energy of activation (ΔG^*) can be solved by using the relation as:

$$\Delta S^* = R \ln\left(\frac{Ah}{K_B T}\right)$$

$$\Delta H^* = E^* - RT$$

$$\Delta G^* = \Delta H^* - T\Delta S^*$$

The thermodynamic and kinetic activation parameters of various decomposition steps of metal complexes are calculated and presented in Table-3. The greater value seen in all the complexes in subsequent steps reflects high thermal stability caused by the covalent bond character. In the first decomposition steps, there is negative entropy of activation which indicates the non-spontaneous dehydration reaction process and positive value of ΔG^* of all complexes indicate the non-spontaneous nature of decomposition steps. The positive value of ΔH^* indicates the endothermic process and the correlation coefficient from the graph indicates a good fit [14,20].

SEM analysis: The SEM images of Zr-TcSal and Pd-TcSal complexes are shown in Fig. 4. Zirconium complex was found to be microcrystalline and nanograins in shape. Similarly, Pd(II) complex showed the agglomeration of hybrid nanomaterial [21,22].

Antibacterial sensitivity: Synthesized metal complexes of mixed ligand were carried out an antimicrobial sensitivity test by Kirby-Bauer paper disc diffusion method and screened *in vitro* of their inhibitory activity against some clinical pathogens with various concentrations (25, 12.5, 6.25 and 3.125 µg/µL). For this test, the calculated amount of metal complex was prepared in DMSO solvent. From the antimicrobial sensitivity study, all the metal complexes show better activity towards tested bacterial pathogens while ligand does not show any effects (Table-4). This result shows that metal complexes have greater activity in comparison to a ligand that indicates the formation of a metal complex where the ligand is bonded with the metal ions. Hence increase in the concentration of metal complexes increases the inhibition zone of bacterial growth [23]. From the presented data, it is clear that zirconium and palladium metal complex shows better results of antibacterial at higher concentrations and goes on decreasing at a lower

TABLE-3
KINETICS AND THERMODYNAMIC PARAMETERS OF ZIRCONIUM(II) AND PALLADIUM(II) METAL COMPLEXES

Complexes	Step	r	A (s⁻¹)	T_{max} (K)	E^* (kJ/mol)	ΔS^* (J/kmol)	ΔH^* (kJ/mol)	ΔG (kJ/mol)
Zr-complex	1	-0.9993	1.68×10^8	355.66	60.311	-88.91	57.354	88.976
	2	-0.9981	2.64×10^{14}	545.88	158.856	26.14	154.318	140.049
	3	-0.9993	7.14×10^{10}	979.71	222.049	-47.02	213.903	259.970
Pd-complex	1	-0.9942	7.30×10^6	470.13	70.608	-117.32	66.699	121.854
	2	-0.9990	2.71×10^{23}	1014.12	4498.82	193.5	4490.378	4294.096
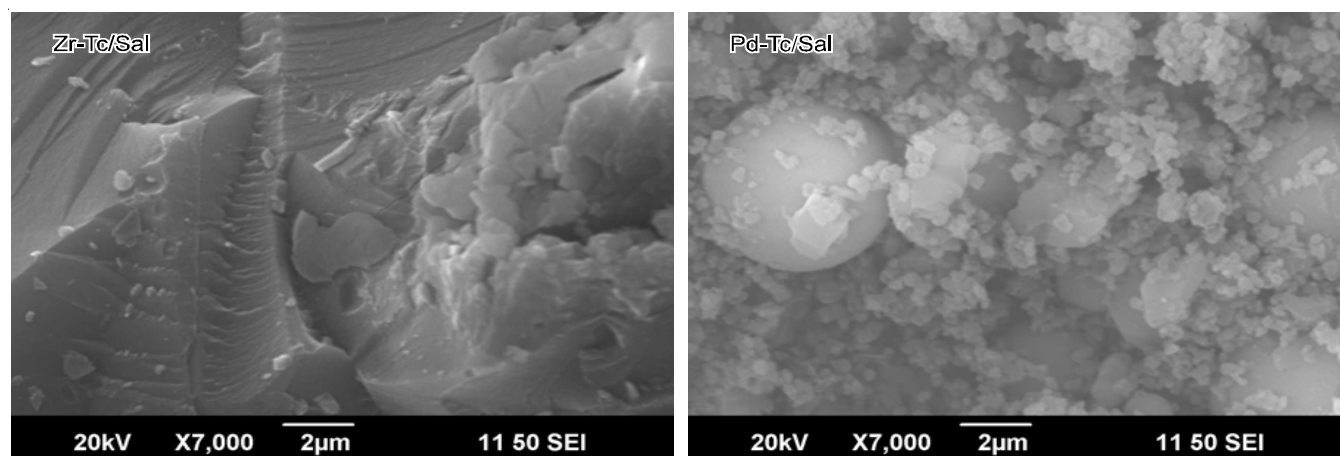
Fig. 4. SEM micrograph of zirconium and palladium complex

TABLE-4
ANTIBACTERIAL GROWTH DATA OF CADMIUM AND MOLYBDENUM METAL COMPLEXES

Complexes	Diameter of zone of inhibition (mm)											
	S. aureus				*P. aeruginosa*				*E. coli*			
Conc. (µg/µL)	25	12.5	6.25	3.125	25	12.5	6.25	3.125	25	12.5	6.25	3.125
Zr-Tc/Sal	12	11	10	9	13	12	10	9	13	12	10	8
Pd-Tc/Sal	26	24	23	22	14	13	12	10	27	24	23	21
Amk (30 mcg/disc)	18				25				28			
Tc	31				31				31			
DMSO	0				0				0			

concentration. *P. aeruginosa* of the zirconium and palladium complex found much less active. Similarly, *E. coli* of palladium complex suggests better results. So all the pathogens had been found susceptible to the synthesized derivatives of tetracycline.

Molecular modeling: The synthesized metal complexes can be structurally characterized based on special designed molecular modeling software by the 3D modeling *via* Chem 3D Pro-12.0 program. In the present study, the proposed structure of metal complexes was carried out. Correct stereochemistry was once finished *via* manipulation and Change to gain low energy molecular geometry. By the MM2 program present in the Cs chem. Office program, the optimized structure of metal complexes were done. The Zr-TcSal and Pd-TcSal have coordinated with tetrahedral and square planar geometry with steric energy of 1719.6070 and 1729.6133 Kcal/mol, respectively. The energy optimization was calculated many times so to obtain the minimum energy of molecular geometry. From the calculation, bond length, bond angles data as well as bonding parameters of Zr-TcSal and Pd-TcSal metal complexes were obtained and are presented in Tables 5 & 6 and their optimized 3D molecular structure is shown in Fig. 5. By the above experimental discussion, the structure of metal complexes of mixed ligand to be proposed. The potential energy will be the sum of all the energy of different types: $E = E_{str} + E_{bend} + E_{tor} + E_{vdw} + E_{oop} + E_{ele}$ where E's denotes energy value for various interaction. The subscripts denote the bond stretching, angle bending, deformation angle, van der Waals interactions, out of plane bending, simple bending and electronic interaction, respectively.

Conclusion

In this present work, the metal complex of zirconium(II) and palladium(II) were successfully synthesized with the help

of tetracycline as primary ligand and salicylaldehyde as the secondary ligand. These complexes had been analyzed by their micro-elemental analysis, FT-IR, (^{1}H & C^{13}) NMR, UV/vis, SEM, TGA/DTA. Molecular modeling signifies the coordination behaviour of metal ions with the ligand and as a result, Zr complex was found to have tetrahedral geometry while Pd complex possesses square planar geometry. All the received results by the above parameters were very much closed to the experimental data. The colour change seen throughout the chemical procedure signifies deprotonation during the formation of the complex. The melting point also indicates the purity of metal complexes. The antimicrobial tests had been done by using Kirby-Bauer paper disc diffusion over metal complexes on three species namely, *Escherichia coli, Pseudomonas aeroginosa (*Gram-negative) and *Staphylococcus aureus* (Gram-positive) with various concentrations (25, 12.5, 6.25 and 3.125 µg/µL) which suggests gorgeous antibacterial activity and comparable sensitivity test of ligand, as well as metal complexes truly, shows that they exhibit strong activity against *E. coli.*

CONFLICT OF INTEREST

The authors declare that there is no conflict of interests regarding the publication of this article.
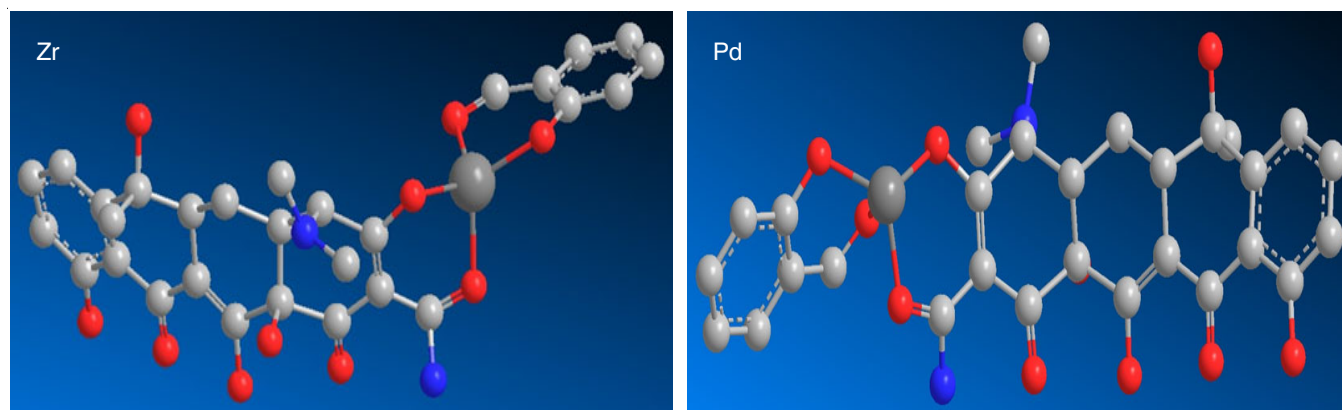
Fig. 5. Molecular modeling of zirconium and palladium complex

TABLE-5 BOND LENGTH AND BOND ANGLE OF Zr COMPLEX					
Atom	Bond length (Å)		Atom	Bond angle (°)	
O(28)-Zr(41)	2.0989		C(33)-C(32)-C(31)	118.9784	
O(25)-Zr(41)	2.0844		C(32)-C(31)-C(30)	118.5948	
O(40)-Zr(41)	2.0968		C(35)-C(30)-C(31)	123.9296	
C(12)-O(42)	1.4195	1.4120	Zr(41)-O(28)-C(26)	110.3553	
O(37)-Zr(41)	2.0831		O(28)-C(26)-N(27)	111.0664	122.6000
C(36)-O(40)	1.2369	1.2080	O(28)-C(26)-C(16)	137.1615	123.0000
C(39)-N(22)	1.4593	1.4380	N(27)-C(26)-C(16)	109.9398	112.7400
N(22)-C(38)	1.4569	1.4380	Zr(41)-O(25)-C(17)	108.7610	
C(35)-O(37)	1.3776	1.3550	C(39)-N(22)-C(38)	108.5503	107.7000
C(34)-C(36)	1.3751	1.5170	C(39)-N(22)-C(18)	112.2253	107.7000
C(35)-C(30)	1.3514	1.4200	C(38)-N(22)-C(18)	115.6873	107.7000
C(34)-C(35)	1.3644	1.4200	N(22)-C(18)-C(13)	113.3836	108.8000
C(33)-C(34)	1.3532	1.4200	N(22)-C(18)-C(17)	113.5587	
C(32)-C(33)	1.3400	1.4200	C(13)-C(18)-C(17)	108.0743	109.5100
C(31)-C(32)	1.3362	1.4200	O(25)-C(17)-C(18)	109.6929	120.0000
C(30)-C(31)	1.3384	1.4200	O(25)-C(17)-C(16)	127.2787	124.3000
C(7)-O(29)	1.2134	1.2080	C(18)-C(17)-C(16)	123.0236	121.4000
C(26)-O(28)	1.2358	1.2080	C(26)-C(16)-C(17)	121.1101	117.6000
C(26)-N(27)	1.3661	1.3690	C(26)-C(16)-C(15)	119.0438	117.6000
C(16)-C(26)	1.3835	1.5170	C(17)-C(16)-C(15)	119.8314	117.6000
C(17)-O(25)	1.3763	1.3550	O(19)-C(15)-C(16)	121.6163	123.0000
C(10)-C(24)	1.5318	1.5140	O(19)-C(15)-C(12)	115.6718	122.5000
C(10)-O(23)	1.4124	1.4030	C(16)-C(15)-C(12)	122.7119	115.0000
C(18)-N(22)	1.4697	1.4380	C(9)-C(14)-C(13)	109.7934	109.5000
C(11)-O(21)	1.3637	1.3550	C(18)-C(13)-C(14)	114.9514	109.5100
C(3)-O(20)	1.3678	1.3550	C(18)-C(13)-C(12)	111.1424	109.5100
C(15)-O(19)	1.2138	1.2080	C(14)-C(13)-C(12)	109.9451	109.5100
C(18)-C(13)	1.5353	1.5230	O(42)-C(12)-C(15)	106.4210	109.5000
C(17)-C(18)	1.5263	1.4970	O(42)-C(12)-C(13)	112.1782	107.5000
C(16)-C(17)	1.3618	1.3370	O(42)-C(12)-C(11)	104.3920	109.5000
C(15)-C(16)	1.3754	1.5170	C(15)-C(12)-C(13)	106.4335	107.8000
C(12)-C(15)	1.5473	1.5090	C(15)-C(12)-C(11)	115.8653	109.4700
C(14)-C(9)	1.5336	1.5230	C(13)-C(12)-C(11)	111.5569	109.4700
C(13)-C(14)	1.5245	1.5230	O(21)-C(11)-C(12)	112.0453	120.0000
C(12)-C(13)	1.5209	1.5140	O(21)-C(11)-C(8)	123.2620	124.3000
C(11)-C(12)	1.5364	1.4970	C(12)-C(11)-C(8)	124.3437	121.4000
C(8)-C(11)	1.3566	1.3370	C(24)-C(10)-O(23)	107.7722	107.5000
C(10)-C(5)	1.5140	1.4970	C(24)-C(10)-C(5)	108.2598	109.4700
C(9)-C(10)	1.5230	1.5140	C(24)-C(10)-C(9)	115.0349	109.4700
C(8)-C(9)	1.5083	1.4970	O(23)-C(10)-C(5)	111.3993	109.5000
C(7)-C(8)	1.3730	1.5170	O(23)-C(10)-C(9)	107.1700	107.5000
C(4)-C(7)	1.3758	1.5170	C(5)-C(10)-C(9)	107.2569	109.4700
C(6)-C(1)	1.3354	1.4200	C(14)-C(9)-C(10)	111.7299	109.5100
C(5)-C(6)	1.3459	1.4200	C(14)-C(9)-C(8)	114.0193	109.5100
C(4)-C(5)	1.3547	1.4200	C(10)-C(9)-C(8)	109.7637	109.5100
C(3)-C(4)	1.3623	1.4200	C(11)-C(8)-C(9)	119.9329	121.4000
C(2)-C(3)	1.3460	1.4200	C(11)-C(8)-C(7)	121.9602	117.6000
C(1)-C(2)	1.3350	1.4200	C(9)-C(8)-C(7)	118.0044	120.0000
Atom	Bond angle (°)		O(29)-C(7)-C(8)	119.9074	123.0000
O(28)-Zr(41)-O(37)	117.4328		O(29)-C(7)-C(4)	118.7473	123.0000
O(25)-Zr(41)-O(40)	116.5393		C(8)-C(7)-C(4)	121.3103	115.0000
O(25)-Zr(41)-O(37)	119.5671		C(1)-C(6)-C(5)	121.0918	
O(40)-Zr(41)-O(37)	97.5287		C(10)-C(5)-C(6)	117.8442	121.4000
Zr(41)-O(40)-C(36)	110.2415		C(10)-C(5)-C(4)	121.2058	121.4000
Zr(41)-O(37)-C(35)	113.1231		C(6)-C(5)-C(4)	120.7592	120.0000
O(40)-C(36)-C(34)	138.2045		C(7)-C(4)-C(5)	120.1926	117.6000
O(37)-C(35)-C(30)	114.6912	124.3000	C(7)-C(4)-C(3)	121.4992	117.6000
O(37)-C(35)-C(34)	128.1872	124.3000	C(5)-C(4)-C(3)	118.2898	120.0000
C(30)-C(35)-C(34)	117.1135	120.0000	O(20)-C(3)-C(4)	126.3191	124.3000
C(36)-C(34)-C(35)	125.4398	117.6000	O(20)-C(3)-C(2)	114.4642	124.3000
C(36)-C(34)-C(33)	116.0640	117.6000	C(4)-C(3)-C(2)	119.1581	120.0000
C(35)-C(34)-C(33)	118.4962	120.0000	C(3)-C(2)-C(1)	122.5248	
C(34)-C(33)-C(32)	122.8864		C(6)-C(1)-C(2)	118.1454	

TABLE-6
BOND LENGTH AND BOND ANGLE OF Pd COMPLEX

Atom	Bond length (Å)		Atom	Bond angle (°)	
O(28)-Pd(41)	1.9186		C(34)-C(33)-C(32)	119.6599	
O(25)-Pd(41)	1.9067		C(33)-C(32)-C(31)	119.7177	
O(40)-Pd(41)	1.9577		C(32)-C(31)-C(30)	119.9319	
C(12)-O(42)	1.4198	1.4120	C(35)-C(30)-C(31)	121.3887	
O(37)-Pd(41)	1.9093		Pd(41)-O(28)-C(26)	110.2716	
C(36)-O(40)	1.2359	1.2080	O(28)-C(26)-N(27)	111.1774	122.6000
C(39)-N(22)	1.4590	1.4380	O(28)-C(26)-C(16)	136.4600	123.0000
N(22)-C(38)	1.4572	1.4380	N(27)-C(26)-C(16)	110.6701	112.7400
C(35)-O(37)	1.3647	1.3550	Pd(41)-O(25)-C(17)	111.2453	
C(34)-C(36)	1.3597	1.5170	C(39)-N(22)-C(38)	108.6976	107.7000
C(35)-C(30)	1.3464	1.4200	C(39)-N(22)-C(18)	112.1732	107.7000
C(34)-C(35)	1.3449	1.4200	C(38)-N(22)-C(18)	115.8804	107.7000
C(33)-C(34)	1.3444	1.4200	N(22)-C(18)-C(13)	113.2471	108.8000
C(32)-C(33)	1.3417	1.4200	N(22)-C(18)-C(17)	113.5017	
C(31)-C(32)	1.3411	1.4200	C(13)-C(18)-C(17)	107.9332	109.5100
C(30)-C(31)	1.3417	1.4200	O(25)-C(17)-C(18)	108.5516	120.0000
C(7)-O(29)	1.2134	1.2080	O(25)-C(17)-C(16)	128.4153	124.3000
C(26)-O(28)	1.2329	1.2080	C(18)-C(17)-C(16)	123.0186	121.4000
C(26)-N(27)	1.3653	1.3690	C(26)-C(16)-C(17)	121.8930	117.6000
C(16)-C(26)	1.3815	1.5170	C(26)-C(16)-C(15)	118.6487	117.6000
C(17)-O(25)	1.3732	1.3550	C(17)-C(16)-C(15)	119.4532	117.6000
C(10)-C(24)	1.5316	1.5140	O(19)-C(15)-C(16)	121.4936	123.0000
C(10)-O(23)	1.4124	1.4030	O(19)-C(15)-C(12)	115.2588	122.5000
C(18)-N(22)	1.4697	1.4380	C(16)-C(15)-C(12)	123.2467	115.0000
C(11)-O(21)	1.3634	1.3550	C(9)-C(14)-C(13)	109.4978	109.5000
C(3)-O(20)	1.3678	1.3550	C(18)-C(13)-C(14)	114.8769	109.5100
C(15)-O(19)	1.2138	1.2080	C(18)-C(13)-C(12)	111.1117	109.5100
C(18)-C(13)	1.5334	1.5230	C(14)-C(13)-C(12)	110.0174	109.5100
C(17)-C(18)	1.5241	1.4970	O(42)-C(12)-C(15)	106.5241	109.5000
C(16)-C(17)	1.3600	1.3370	O(42)-C(12)-C(13)	112.3297	107.5000
C(15)-C(16)	1.3761	1.5170	O(42)-C(12)-C(11)	104.3594	109.5000
C(12)-C(15)	1.5485	1.5090	C(15)-C(12)-C(13)	106.6587	107.8000
C(14)-C(9)	1.5334	1.5230	C(15)-C(12)-C(11)	116.0118	109.4700
C(13)-C(14)	1.5246	1.5230	C(13)-C(12)-C(11)	110.9949	109.4700
C(12)-C(13)	1.5207	1.5140	O(21)-C(11)-C(12)	112.2028	120.0000
C(11)-C(12)	1.5372	1.4970	O(21)-C(11)-C(8)	123.1081	124.3000
C(8)-C(11)	1.3568	1.3370	C(12)-C(11)-C(8)	124.3046	121.4000
C(10)-C(5)	1.5141	1.4970	C(24)-C(10)-O(23)	107.8185	107.5000
C(9)-C(10)	1.5226	1.5140	C(24)-C(10)-C(5)	108.3483	109.4700
C(8)-C(9)	1.5085	1.4970	C(24)-C(10)-C(9)	115.0343	109.4700
C(7)-C(8)	1.3730	1.5170	O(23)-C(10)-C(5)	111.3898	109.5000
C(4)-C(7)	1.3759	1.5170	O(23)-C(10)-C(9)	107.1622	107.5000
C(6)-C(1)	1.3354	1.4200	C(5)-C(10)-C(9)	107.1377	109.4700
C(5)-C(6)	1.3458	1.4200	C(14)-C(9)-C(10)	111.8702	109.5100
C(4)-C(5)	1.3548	1.4200	C(14)-C(9)-C(8)	114.0879	109.5100
C(3)-C(4)	1.3623	1.4200	C(10)-C(9)-C(8)	109.7362	109.5100
C(2)-C(3)	1.3460	1.4200	C(11)-C(8)-C(9)	120.0652	121.4000
C(1)-C(2)	1.3350	1.4200	C(11)-C(8)-C(7)	121.9652	117.6000

Atom	Bond angle (°)		Atom	Bond angle (°)	
O(28)-Pd(41)-O(25)	105.4056		C(9)-C(8)-C(7)	117.8666	120.0000
O(28)-Pd(41)-O(40)	77.2374		O(29)-C(7)-C(8)	119.8504	123.0000
O(28)-Pd(41)-O(37)	120.9912		O(29)-C(7)-C(4)	118.8096	123.0000
O(25)-Pd(41)-O(40)	76.0215		C(8)-C(7)-C(4)	121.3014	115.0000
O(25)-Pd(41)-O(37)	118.4376		C(1)-C(6)-C(5)	121.0809	
O(40)-Pd(41)-O(37)	77.3124		C(10)-C(5)-C(6)	117.8315	121.4000
Pd(41)-O(40)-C(36)	110.3238		C(10)-C(5)-C(4)	121.2188	121.4000
Pd(41)-O(37)-C(35)	111.9655		C(6)-C(5)-C(4)	120.7695	120.0000
O(40)-C(36)-C(34)	128.9963		C(7)-C(4)-C(5)	120.1932	117.6000
O(37)-C(35)-C(30)	122.0481	124.3000	C(7)-C(4)-C(3)	121.4998	117.6000
O(37)-C(35)-C(34)	120.1909	124.3000	C(5)-C(4)-C(3)	118.2888	120.0000
C(30)-C(35)-C(34)	117.7490	120.0000	O(20)-C(3)-C(4)	126.3340	124.3000
C(36)-C(34)-C(35)	116.3097	117.6000	O(20)-C(3)-C(2)	114.4593	124.3000
C(36)-C(34)-C(33)	122.1389	117.6000	C(4)-C(3)-C(2)	119.1485	120.0000
C(35)-C(34)-C(33)	121.5510	120.0000	C(3)-C(2)-C(1)	122.5329	
			C(6)-C(1)-C(2)	118.1487	

REFERENCES

1. P.H. Chang, W. Jiang, Z. Li, J. Jean and C.Y. Kuo, *Res. & Rev.:J. Pharm. Anal.*, **4**, 86 (2015).

2. T.K. Pal, M.A. Alam and S.R. Paul, *J. Bangladesh Acad. Sci.*, **34**, 153 (1970);
    https://doi.org/10.3329/jbas.v34i2.6859

3. S. Shobana, P. Subramaniam, L. Mitu, J. Dharmaraja and S. Arvind Narayan, *Spectrochim. Acta A Mol. Biomol. Spectrosc.*, **134**, 333 (2015);
    https://doi.org/10.1016/j.saa.2014.06.093

4. A.A. Soliman, S.A. Ali, A.H. Marei and D.H. Nassar, *Spectrochim. Acta A Mol. Biomol. Spectrosc.*, **89**, 329 (2012);
    https://doi.org/10.1016/j.saa.2011.12.061

5. N. Qamar, H. Sultan, M. Khan, R. Azmat, R. Naz, A. Hameed and M. Lateef, *ChemSelect*, **4**, 3058 (2019);
    https://doi.org/10.1002/slct.201803882

6. H.F.A. El-Halim, G.G. Mohamed, M.M.I. El-Dessouky and W.H. Mahmoud, *Spectrochim. Acta A Mol. Biomol. Spectrosc.*, **82**, 8 (2011);
    https://doi.org/10.1016/j.saa.2011.05.089

7. Y. Zhao, Y. Tan, Y. Guo, X. Gu, X. Wang and Y. Zhang, *Environ. Pollut.*, **180**, 206 (2013);
    https://doi.org/10.1016/j.envpol.2013.05.043

8. J.A. Anderson, P.W. Groundwater., A. Todd and A.J. Worsley, *Pharm. J.*, **283**, 359 (2004).

9. J.A. Obaleye, O.O. Abosede, A.S. Kumbhar and N. Olusola, *Can. Chem. Trans.*, **4**, 168 (2016);
    https://doi.org/10.13179/canchemtrans.2016.04.02.0257

10. M. M. El-Ajaily, H.A. Abdullah, A. Al-Janga, E.E. Saad and A.A. Maihub, *Adv. Chem.*, **2015**, 987420 (2015);
    https://doi.org/10.1155/2015/987420

11. W.H. El-Shwiniy, W.S. Shehab, S.F. Mohamed and H.G. Ibrahium, *Appl. Organomet. Chem.*, **32**, e4503 (2018);
    https://doi.org/10.1002/aoc.4503

12. K. Sharma, R.V. Singh and N. Fahmi, *Spectrochim. Acta A Mol. Biomol. Spectrosc.*, **78**, 80 (2011);
    https://doi.org/10.1016/j.saa.2010.08.076

13. H.L. Singh and J. Singh, *Int. J. Inorg. Chem.*, **2013**, 847071 (2013);
    https://doi.org/10.1155/2013/847071

14. I.M.I. Moustafa and M.H. Abdellattif, *Mod. Chem. Appl.*, **5**, 202 (2018);
    https://doi.org/10.4172/2329-6798.1000202

15. B.S. Prakash, C.I.S. Raj and R.G. Allen Gana, *J. Eng. Sci.*, **6**, 43 (2017).

16. H. Khan, A. Badshah, M. Said, G. Murtaza, J. Ahmad, B.J. Jean-Claude, M. Todorova and I.S. Butler, *Appl. Organomet. Chem.*, **27**, 387 (2013);
    https://doi.org/10.1002/aoc.2991

17. N. Rathee and K.K. Verma, *J. Serb. Chem. Soc.*, **77**, 325 (2012);
    https://doi.org/10.2298/JSC101211200R

18. L. Tabrizi, H. Chiniforoshan and H. Tavakol, *Spectrochim. Acta A Mol. Biomol. Spectrosc.*, **141**, 16 (2015);
    https://doi.org/10.1016/j.saa.2015.01.027

19. H.G. Aslan, S. Özcan and N. Karacan, *Inorg. Chem. Commun.*, **14**, 1550 (2011);
    https://doi.org/10.1016/j.inoche.2011.05.024

20. N.K. Chaudhary and P. Mishra, *Bioinorg. Chem. Appl.*, **2017**, 6927675 (2017);
    https://doi.org/10.1155/2017/6927675

21. T.K. Pal, M.A. Alam, S. Paul and M.C. Sheikh, *J. King Saud Univ. Sci.*, **31**, 445 (2017);
    https://doi.org/10.1016/j.jksus.2017.12.010

22. M. Díaz-Sánchez, D. Díaz-García, S. Prashar and S. Gómez-Ruiz, *Environ. Chem. Lett.*, **17**, 1585 (2019);
    https://doi.org/10.1007/s10311-019-00899-5

23. H.A. EL-Ghamry, K. Sakai, S. Masaoka, K.Y. El-Baradie and R.M. Issa, *Chin. J. Chem.*, **30**, 881 (2012);
    https://doi.org/10.1002/cjoc.201280024